OPEN

PRS GLOBAL OPEN EXPERIMENTAL

Effect of Systemic Adipose-derived Stem Cell Therapy on Functional Nerve Regeneration in a Rodent Model

Riccardo Schweizer, MD*†‡
Jonas T. Schnider, MD*†
Paolo M. Fanzio, MD*†
Wakako Tsuji, MD, PhD*†
Nataliya Kostereva, PhD*†
Mario G. Solari, MD*†
Jan A. Plock, MD*†‡
Vijay S. Gorantla, MD, PhD†§

Background: Regardless of etiology, peripheral nerve injuries (PNI) result in disruption/loss of neuromuscular junctions, target muscle denervation, and poor sensorimotor outcomes with associated pain and disability. Adipose-derived stem cells (ASCs) have shown promise in neuroregeneration. However, there is a paucity of objective assessments reflective of functional neuroregeneration in experimental PNI. Here, we use a multimodal, static, and dynamic approach to evaluate functional outcomes after ASC therapy in a rodent PNI model.

Methods: Lewis rats were divided into 3 groups: 10 mm sciatic nerve resection ("CUT" group; n = 10), transection and repair ("REP" group; n = 10), transection and repair plus single-dose ASCs ("ASC" group; n = 12). Allogeneic (Brown Norway rat) ASCs (1×10^6) were administered intravenously on postoperative day 1. Functional outcome was assessed by static sciatic index, toe spread factor, and a dynamic swim test on a weekly basis for 6 weeks. Sciatic nerves and gastrocnemius muscles were harvested at endpoint (6 weeks) for histological analysis.

Results: The ASC group showed accelerated functional recovery on the swim test at 2 weeks postoperatively, with continued improvement over 4 weeks, culminating in superior overall outcomes at 6 weeks compared with the REP group. The CUT group showed no significant improvement from baseline. Nerve histomorphometry correlated well with the swim test results in the ASC group. Gastrocnemius muscle weights showed no difference between the REP and the ASC groups.

Conclusion: Our study confirms that early, single dose, systemic administration of ASC after PNI accelerates and enhances overall motor recovery on static and dynamic functional tests as evidenced by improvements in voluntary as well as involuntary motions. *(Plast Reconstr Surg Glob Open 2020;8:e2953; doi: 10.1097/GOX.0000000000002953; Published online 21 July 2020.)*

INTRODUCTION

Peripheral nerve injury (PNI) has an incidence of 3%–5% in the United States.[1,2] PNI results from trauma, compression (tunnel syndromes), or iatrogenic causes.[2,3] The resultant motor or sensory loss of function, and unmanageable neuropathic pain, can all result in significant treatment costs and limited quality of life. Treatment approaches remained relatively unchanged throughout the past 50 years.[4]

Even with best surgical apposition, approximately only 10% of axons reach the target organs after nerve transection.[5,6] The speed and quality of overall axonal regeneration is critical for neurofunctional outcomes, as prolonged denervation of the target muscles leads to a poor outcome—for example, loss of motor endplates and muscular atrophy.

*From the *Department of Plastic Surgery, University of Pittsburgh Medical Center (UPMC), Pittsburgh, Pa.; †McGowan Institute for Regenerative Medicine, University of Pittsburgh, Pittsburgh, Pa.; ‡Division of Plastic Surgery and Hand Surgery, University Hospital Zurich (USZ), Switzerland; and §Departments of Surgery, Ophthalmology and Bioengineering, Wake Forest University Health Sciences, Wake Forest Institute for Regenerative Medicine, Winston Salem, N.C.*

Received for publication April 8, 2020; accepted May 7, 2020.

DOI: 10.1097/GOX.0000000000002953

Disclosure: *The authors have no financial interest to declare in relation to the content of this article. This study was made possible by the generous support of the Department of Defense—Congressionally Directed Medical Research Program Grant Funding (W81XWH-11-2-0215 and W81XWH-15-2-0061; PI: Vijay Gorantla). In addition, Drs. Schweizer and Schnider were recipients of Swiss National Science Foundation funding.*

Related Digital Media are available in the full-text version of the article on www.PRSGlobalOpen.com.

Treatment paradigms in experimental PNI models ranged from neurotrophic agents (drugs/biologics/growth factors) to cell therapies such as Schwann cells or bone marrow or adipose-derived mesenchymal stem cells (ASCs).[7–13] Characteristics of ASCs such as ease of procurement, negligible donor site morbidity, and higher yields than other sources of mesenchymal stem cells (MSCs) make them ideally suited for local or systemic neurotherapies.[8,14–19]

An ideal functional test to investigate true efficacy of neurotherapies must be easy to perform, repeatable and reproducible, and objective with low biases and confounders. Traditional qualitative/functional assessment in experimental PNI such as gait analysis [walking track, CatWalk (CatWalk XT 10, Noldus Information Technology, Wageningen, The Netherlands), treadmills] only measure voluntary activity that depends on subject motivation. Alternative assessments such as the swim test, which use swimming as a natural, involuntary behavior and eliminate confounders of traditional gait analyses, could be better reflective of qualitative functional neuro-behavioral outcomes after PNI. Swim test has not been tested in PNI and may complement gold-standard quantitative metrics of regeneration such as histomorphometry.[20,21] Here we present the first attempt to evaluate a single dose, systemically administered, ASC-based neurotherapy protocol in a rodent sciatic nerve cut/repair model to facilitate axonal regeneration and improve the functional outcomes in PNI.

MATERIALS AND METHODS

This study was conducted in compliance with the University of Pittsburgh Institutional Animal Care and Use Committee (IACUC) and Association for Assessment and Accreditation of Laboratory Animal Care (AALAC) guidelines.

ASC Isolation, Cultivation, and Characterization

ASCs isolated from adipose tissues excised from inguinal fat pads and bilateral epididymes of rats were digested with collagenase type II (Worthington Biochemical Corp, Lakewood, N.J.) and bovine serum albumin (Millipore, Billerica, Mass.) in Hanks' balanced solution (Cellgro Mediatech Inc., Manassas, Va.) for 60 minutes at 37°C while shaking. After washing and treatment with erythrocyte lysis buffer, the cells were filtered through a sterile gauze. The pellet was transferred to culture flasks with Dulbecco's modified Eagle's medium (Cellgro Mediatech) plus supplemental Ham's F-12 medium (Gibco, Grand Island, N.Y.). After 6 hours, nonadherent cells were washed out, retaining only adherent ASCs. Cells were cultured in Dulbecco's modified Eagle's medium/F12 with 10% fetal bovine serum (ATLAS Biologicals, Fort Collins, Colo.), 0.1 μM dexamethasone (Sigma-Aldrich, St. Louis, Mo.), 1% penicillin-streptomycin.[22] ASC surface marker phenotype was negative for CD45 and positive for CD29, CD73 and CD90 as found by flow cytometry (FACS Aria, Becton Dickinson).[23]

Animals and Experimental Protocol

Male Lewis rats (6–8 weeks, 250–300 g; Harlan Labs, Indianapolis, Ind.) were randomly assigned to 3 groups: (1) 10 mm sciatic nerve resection without repair ("CUT" group; n = 10); (2) sciatic nerve transection and repair ("REP" group; n = 10); (3) sciatic nerve transection and repair with single-dose systemic ASC therapy ("ASC" group; n = 12). Buprenorphine was administered (0.05 mg/kg, 3–4 times per day) for analgesia.

Static sciatic index (SSI) and toe spread factor (TSF) were used for static (unenforced) functional assessment, and the swim test was used to assess dynamic (forced) function. All animals underwent behavioral conditioning for 2–3 weeks before surgery. Training swim sessions were conducted with the goal of 3 complete swims per session. Following baseline (BL) measurements, testing was continued until 6 weeks (Fig. 1).

A

Group	n	Intervention	Cell Therapy
CUT	10	Sciatic nerve resection (10mm)	None
REP	10	Sciatic transection and repair	None
ASC	12	Sciatic transection and repair	1x10^6 ASCs i.v. on POD 1

Table 1. Experimental groups, intervention and therapy.
ASCs = adipose-derived stem cells; POD = postoperative day.

B

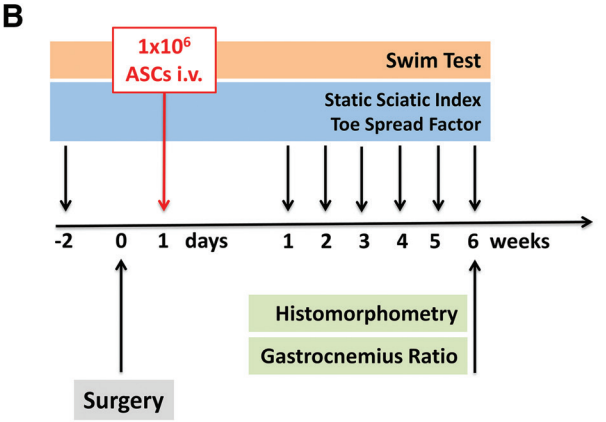

Fig. 1. Experimental groups and protocol. A, Table summarizing the experimental groups with surgical interventions and cell therapy. B, Experimental protocol showing the interventions and assessments on a timeline.

Surgical Procedure

Rats were anesthetized with 2% isoflurane (100% oxygen flow at 1 L/min), (VetEqiup; Pleasanton, Calif.). Legs were shaved, prepared, and draped, and the right sciatic nerve was exposed via dorsolateral incision between biceps femoris and gluteus muscle. In the CUT group, a 10 mm sciatic nerve segment was resected before its bifurcation into peroneal branch to hinder nerve regeneration (the segment ending 5 mm proximal to peroneal branching). This zone contains motor fibers (for functional return) and also cutaneous afferent fibers that are key to pain sensation and proprioception.[24] The REP/ASC groups underwent sciatic nerve transection at same level as the CUT group, followed by microsurgical epineural neurorrhaphy with 9-0 nylon sutures at 10 mm

proximal to branching. The skin was closed with interrupted resorbable sutures.

Static Functional Assessment

The SSI and TSF assess functional motor deficits in the peroneal and tibial branches of the sciatic nerve.[25] Animals were placed on a transparent plexiglass walkway, ensuring that all 4 limbs uniformly touched the surface. High-resolution photographs of paw patterns were obtained from below with a camera positioned perpendicular to the glass surface at fixed distance and zoom. Toe 1–5 (toe spread) and toe 2–4 (intermediate toe spread) distances were measured in the operated-on (O, right) and naive legs (N, left) to calculate TSF and intermediate toe spread factor (ITSF) as follows: TSF = (OTSF – NTSF)/NTSF; ITSF = (OITSF – NITSF)/NITSF. The SSI was calculated as described previously: SSI = 108.44(TSF) + 31.85(ITSF) – 5.49.[25] (**See figure, Supplemental Digital Content 1**, which displays toe spread factor measurement. Representative depiction of TSF measurement: the right paw has lost its intrinsic ability for toe spread 1 week after sciatic nerve resection. In comparison, the uninjured, naive left paw shows normal toe spread (toe spread, red line) and intermediate toe spread (intermediate toe spread, blue line). ****P < 0.0001 by 2-way analysis of variance (ANOVA) with Tukey's multiple comparisons, **http://links.lww.com/PRSGO/B422**.)

Dynamic Functional Assessment

Animals underwent weekly swim sessions starting 1 week postoperatively. The setup consisted of a water-filled plexiglass tank (70 × 25 × 40 cm^3; 27°C–30°C) with a metallic ladder (Fig. 2A). A high-resolution, cine-camera (GoPro Hero 2; Go Pro Inc., San Mateo, Calif.) was placed parallel to long axis of the tank on a tripod at 100 cm distance with 0-degree vertical and horizontal lens tilt at water level. High-frame (120 fps) videos were captured, including the middle 50 cm section of the tank. Each swim was calculated by 3 consecutive swims for a total of 150 cm. Swims were considered valid if the animal swam without hesitation from the yellow starting line to the exit grid. Recordings were analyzed offline for number of strokes observed in the injured hindlimb per swim, working angle covered during each stroke, and time per swim. Working angle was measured using a free shareware (Onde Rulers v1.12.1, Mac Update, Mich.) superimposing a goniometer directly onto the video at the selected still frame (Fig. 2B). The exact range of motion (ie, working angle) was calculated based on the angulation between the horizontal water line and the degree of motion of mid-foot from the anterior to posterior position during each stroke. A performance score (PS) was calculated by dividing strokes per run by time for the run: PS = (strokes per run)/(time per run) × 1000. All image and video measurements were performed by one researcher (P.M.F.) blinded to the groups.

Gastrocnemius Muscle Ratio

The gastrocnemius muscles were harvested bilaterally at endpoint, and the ratio of muscle weight on the side that was operated on versus the contralateral (naive) side determined the degree of muscle atrophy.

Immunohistochemistry and Histomorphometry

Nerve samples 10 mm distal to the coaptation site were fixed in Bouin's solution and processed as described earlier.[26] After blocking with normal serum, 10-µm-thick sections were incubated with the first antibody (neurofilament medium chain; 1:400; ThermoScientific/Pierce, Waltham, Mass.) and counterstained with Hoechst 33258 (nucleus) and FluoroMyelin (Sigma-Aldrich). Whole nerve cross-sections were imaged with a Nikon 90i microscope (40×). Fiber density (fibers/mm^2), total number of fibers per distal area of nerve, myelin area, axon area, and G-ratio (axon diameter/nerve diameter) were calculated in photomicrographs using MetaMorph software (Molecular Devices LLC, San Jose, Calif.). Six random regions of interest of myelinated nerve fibers (covering 80%–90% of the nerve cross-section) were blindly analyzed in each nerve section.

Statistical Analysis

Prism 8.0 (GraphPad Software, La Jolla, Calif.) was used for statistical analysis. Data are presented as mean ± SD unless otherwise indicated. Differences between the groups were assessed by 2-way ANOVA (SSI, TSF, Swim Test) with Tukey's multiple comparisons between groups and timepoints. Gastrocnemius ratios were compared with 1-way ANOVA and Bonferroni's multiple comparison posttest. Kruskal–Wallis Test with Dunn's multiple comparison posttest was used for histomorphometry data. A value of $P < 0.05$ was chosen to represent statistical significance.

RESULTS

All animals that were operated on reached the endpoint with no complications such as wound breakdown or infections and demonstrated proper weight gain over the 6 weeks. **(See figure, Supplemental Digital Content 2**, which displays rat weights. Rats were weighed regularly over the time frame of the experiment, here BL, 4 weeks, and 6 weeks values are provided for the different groups. Not significant difference was noticed between the groups, **http://links.lww.com/PRSGO/B423**.) The animals receiving cell injections had no adverse events in terms of embolic complications or sudden death.

Static Functional Assessment

A significant drop in both SSI and TSF was observed at week 1 compared with that at BL (Fig. 3). SSI for the CUT, REP, and ASC groups at week 1 was –105.92 ± 4.02, –108.76 ± 7.34, and –104.47 ± 8.54 versus preoperative –2.91±7.04 (all groups $P < 0.001$). The CUT group had no improvement the following 6 weeks (–103.37 ± 6.94), while the REP and ASC groups revealed progressive improvement, culminating in –71.91 ± 16.76 and –46.03 ± 13.66 at week 6 ($P < 0.0001$ REP versus ASC; $P < 0.0001$

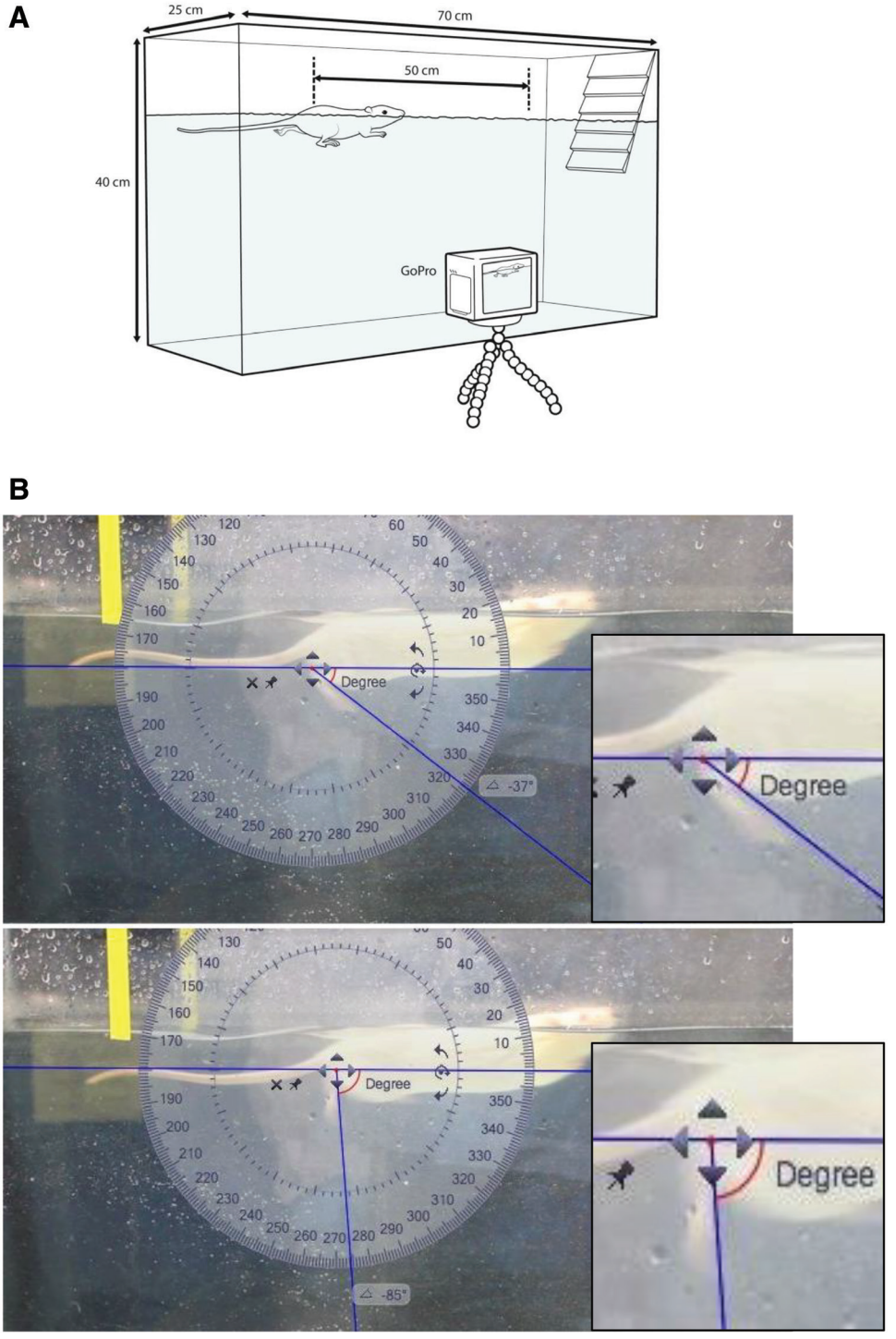

Fig. 2. Swim test setup and measurement. A, A tank measuring 70 × 40 × 25 cm^3 (length × height × width) with a metallic grid at one end for entry/exit by animals was used for the dynamic (forced function) tests. The tank was filled with warm tap water (27°C–30°C) to a depth of 30 cm for each swim run. The tank was cleaned and water regularly changed after each run. The swims were recorded at 30 frames/s by a GoPro HERO 7 camera in front of the tank at a defined distance to record the central 50 cm length of the swim. B, The recorded videos were analyzed offline, and the working angles of the right paw during swim test were measured on single frames (as illustrated). The working angle was measured by drawing a line over the mid foot and one on the water surface (for both the most anterior and the most posterior part of the cycle, calculating the Δ).

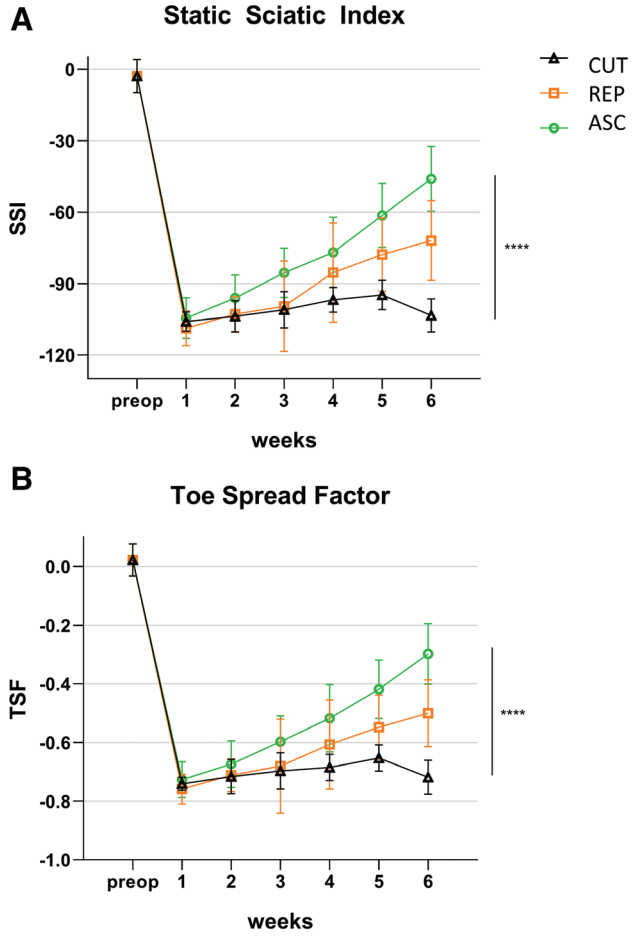

Fig. 3. Static functional tests. Both SSI (A) and TSF (B) tests were performed before the dynamic swim testing for evaluating unenforced function. The SSI adequately reflected surgical nerve injury 1 week postoperatively in all groups. Both the REP and ASC groups showed a significant improvement in SSI at week 6 compared with the CUT group, which did not show significant improvement. A similar result was obtained for TSF. ASC, transection and repair with ASC therapy; CUT, resection with no repair; REP, transection and repair.

versus CUT). The ASC group had significantly higher SSI recovery compared with the REP group from week 3 to endpoint ($P < 0.0001$ at 6 weeks). Similarly, TSF for the CUT, REP, and ASC groups were −0.74 ± 0.02, −0.75 ± 0.05 and −0.72 ± 0.06 compared with BL CUT group values of 0.02 ± 0.05 at week 1. At endpoint, ASC showed the best improvement (−0.29 ± 0.10 versus −0.50 ± 0.11 for the ASC group and −71 ± 0.05 for the CUT group; $P <$ 0.0001 for all groups).

Dynamic Functional Assessment

All groups showed a clear drop in overall forced function on the swim test (stroke number, working angle, and PS; Fig. 4) compared with preoperative values [BL, 17.46 ± 2.70 versus 10.83 ± 0.98 (CUT), 10.17 ± 0.40 (REP), and 12.00 ± 0.93 (ASC) at week 1 ($P < 0.001$); $P > 0.05$ between groups at week 1; all groups $P < 0.0001$ versus BL; Fig. 4]. ASC showed early improvement in stroke number versus REP at week 2 (14.37 ± 1.68 versus 11.83 ± 0.40; $P < 0.01$), but values at endpoint were comparable [15.5 ± 1.05 (REP) versus 15.71 ± 1.8 (ASC); $P > 0.05$]. Stroke number remained poor in CUT versus REP/ASC groups (11.17 ± 0.75 at week 6, $P < 0.0001$ versus REP/ASC).

Overall swim duration was prolonged in all experimental groups with no intergroup difference (CUT group, 4695 ± 288; REP group, 4784 ± 221; ASC group, 5273 ± 555 versus BL, 3295 ± 491 ms; $P > 0.05$). However, recovery in the REP and ASC groups was significantly superior to that in the CUT group (REP, 4256 ± 364 and ASC, 3428 ± 332 versus CUT, 5383 ± 546) over the following 6 weeks, with most discernible improvements after week 3 ($P < 0.01$ REP versus ASC; ASC $P < 0.0001$ week 1 versus week 6).

Working angles dropped to 35.33 ± 7.34 degrees (CUT), 46.58 ± 8.01 degrees (REP), and 49.56 ± 3.14 degrees (ASC) at week 1 versus that at BL (100.78 ± 4.61 degrees, $P < 0.0001$ BL versus week 1; $P > 0.05$ all groups at week 1). The REP and ASC groups showed slight improvement over 6 weeks, reaching significance ($P < 0.0001$) in ASC at week 6 compared with week 1, while the CUT group remained at values similar to that at week 1 (CUT, 33.75 ± 7.21 degrees; REP, 49.25 ± 9.33 degrees; ASC, 49.25 ± 9.33 degrees at week 6; $P < 0.001$ between groups).

Overall PS also showed an initial drop compared to that at BL (5.40 ± 0.67), but from 2 to 6 weeks, scores in the REP and ASC groups were significantly higher than that at the CUT group (ASC > REP at endpoint). Scores for the CUT, REP, and ASC groups were 2.31 ± 0.23, 2.14 ± 0.16, and 2.29 ± 0.25 at week 1 and 2.13 ± 0.40 (CUT), 3.64 ± 0.16 (REP), 4.61 ± 0.65 (ASC) at week 6 (REP $P >$ 0.05 and ASC $P < 0.001$ versus week 1; $P < 0.001$ REP versus ASC; $P < 0.0001$ ASC versus CUT).

Gastrocnemius Muscle Ratio

Gastrocnemius muscle ratios at endpoint were significantly higher in the REP and ASC group compared with the CUT group (REP, 0.43 ± 0.05; ASC, 0.41 ± 0.09; CUT, 0.24 ± 0.02; $P < 0.001$; Fig. 5). There was no significant difference between REP and ASC at endpoint.

Histomorphometry

Distal to site of injury/coaptation, nerve fiber density, axon area, and myelin area showed significantly higher mean values in ASC compared with the REP group at week 6, with no significant trend observed in total fiber number (Fig. 6). The G-ratio as marker for nerve maturity revealed no difference between the ASC and the REP groups [0.668 ± 0.040 (REP), 0.672 ± 0.036 (ASC) and 0.745 ± 0.032 (naive); $P > 0.05$ ASC versus REP]. Nerve fiber density was 10,303 ± 4038 for REP, 14,042 ± 4325 for ASC, and 12,627 ± 1808 fibers/mm^2 for naive ($P < 0.0001$ REP versus ASC), and total fiber numbers were 2666 ± 1555 (REP), 6486 ± 471.6 (ASC), and 4911 ± 2919 (naive) ($P > 0.05$ REP versus ASC). Axon and myelin cross-section areas were 3.68 ± 2.20 (REP), 4.99 ± 2.92 (ASC), and 12.50 ± 6.66 μm^2 (naive) ($P < 0.001$ REP versus ASC) and 13.80 ± 5.88 (REP), 19.41 ± 6.54 (ASC), and 52.82 ± 21.63 μm^2 (naive) ($P < 0.0001$ REP versus ASC), respectively.

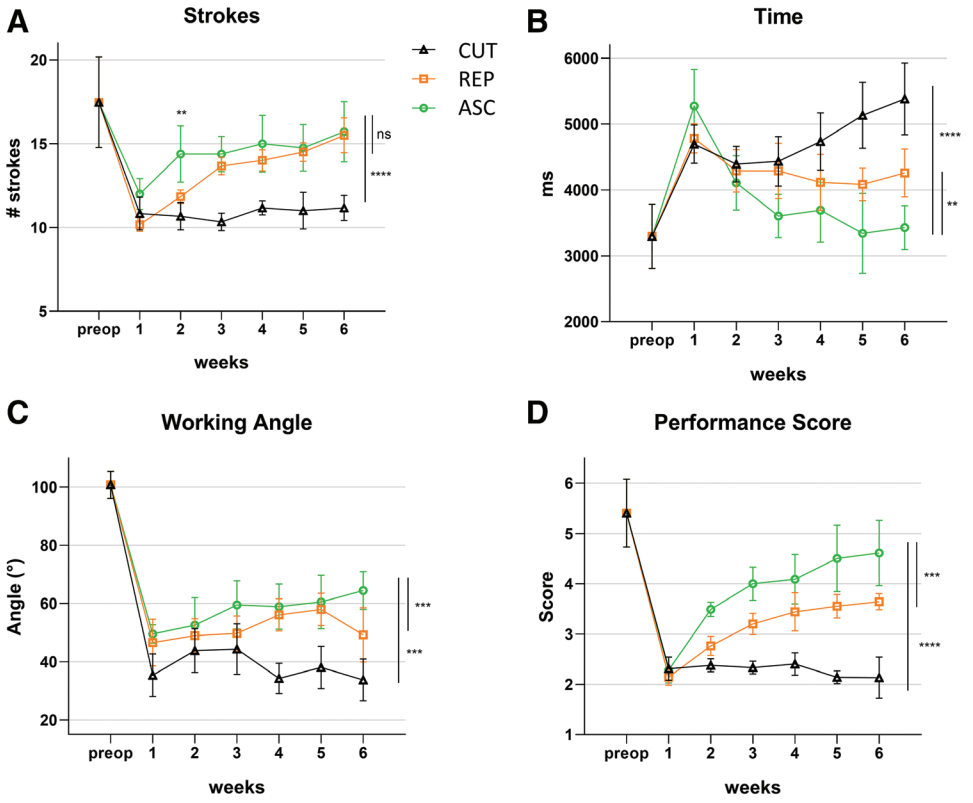

Fig. 4. Dynamic swim test. Four parameters were analyzed offline from the recorded swim tests: strokes per swim (A), time to complete the swim run (ms; B), working angle (degree; C), and performance score (D). Functional deficits secondary to the intervention were detectable as early as week 1. Animals in the CUT group took significantly longer time to perform the swim runs than those in the REP/ASC group at 6 weeks. Working angle was significantly higher in the ASC group compared with those in the REP and CUT groups at 6 weeks. The ASC group demonstrated a higher overall number of strokes at 1–2 weeks compared with the REP group, suggesting an accelerated functional recovery by ASCs. The REP group showed similar results as the ASC group at 6 weeks. The performance score was significantly higher in the ASC group compared with the REP and CUT groups at 6 weeks. $^{**}P < 0.01$, $^{***}P < 0.001$, $^{****}P < 0.0001$ by 2-way ANOVA with Tukey's multiple comparisons.

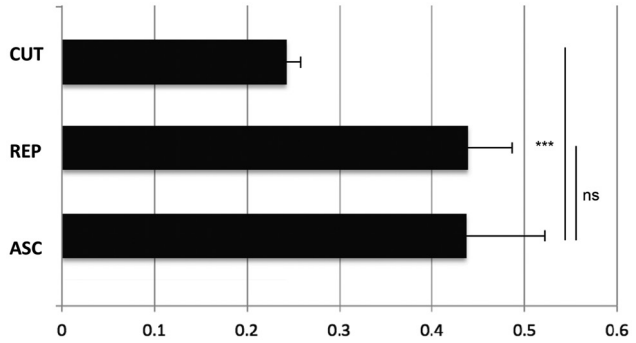

Fig. 5. Gastrocnemius muscle ratio. Gastrocnemius muscles from the operated and the naive side were recovered and weighed at study end point, and a ratio of the wet muscle weights on the operated versus naive limbs was calculated. Gastrocnemius ratios were significantly higher in the REP/ASC group compared with the CUT group. No difference was noted between the repaired groups at endpoint. $^{***}P < 0.001$ by 1-way ANOVA and Bonferroni's multiple comparison posttest.

DISCUSSION

Since recognition of the therapeutic potential of MSCs, and in particular ASCs,[19,27–29] numerous studies have investigated their putative positive effects in spinal cord injury and PNI.[30–32] While the current body of knowledge supports both trans-differentiation to Schwann cell[33] or paracrine effects via neurotropic and neurotrophic factors[34–36] as possible mechanisms, a combination of both might hold true.[37,38] Most studies performed have explored efficacy of ASCs administered locally,[15] seeded in conduits,[8,14,17,39,40] or deposited in gels,[41] rather than incorporating ASC-derived neurospheres, exosomes, or conditioned media.[15,42]

Prior studies have shown positive effects of systemic MSCs or ASCs in modulating tissue inflammation and nerve injury.[43–45] Given the high probability of lung entrapment, we believe the positive functional effects in the current study were secondary to paracrine effects, as in earlier studies in other models.[46,47] Paracrine effects of ASC in PNI could involve neurotropic and neurotrophic factors acting directly on the regenerating nerve and being permissive for a regenerative milieu, favoring SCs action.[34–36] Indeed, neurotrophic factors such as brain-derived neurotrophic factor, nerve growth factor, and glial-derived

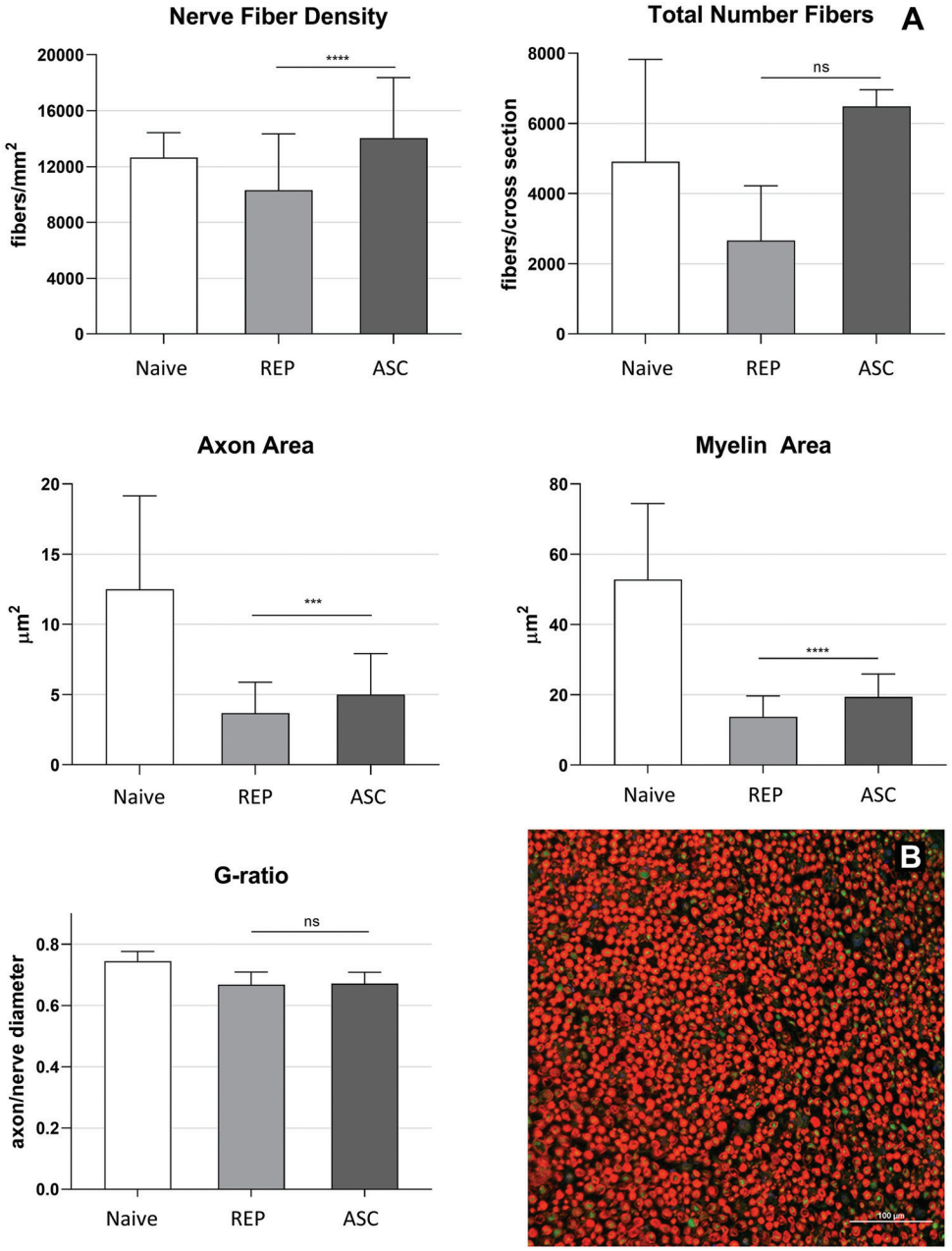

Fig. 6. Histomorphometric nerve analysis. Nerve samples were procured at endpoint and for analysis of multiple morphologic parameters: fiber density (A), number of fibers per cross-section (B), axon area (C), myelin area (D), and G-ratio (E, axon diameter/nerve diameter). The ASC group exhibited significantly higher values for all the parameters except for G-ratio. Values in the contralateral naive sciatic nerve were used for baseline reference comparison. ***$P < 0.001$, **** $P < 0.0001$ by Kruskal-Wallis test with Dunn's multiple comparison posttest. F, Representative cross section of the sciatic nerve as measured by MetaMorph Software (Molecular Devices LLC, San Jose, Calif.) to assess nerve fiber density and myelinization (red, myelin; green, axon).

neurotrophic factor secreted or upregulated by ASCs augment axonal regrowth and myelination.[36,48,49]

The resection group had a significantly lower gastrocnemius ratio, indicating muscle atrophy as seen by others.[50] However, significantly higher values in the treated groups point to the benefit of ASC and simple repair in preventing atrophy.[15,51] The SSI scores with early single-dose ASC treatment were superior to the results from crush studies with late administration (after 6 weeks), alluding to an immunomodulatory effect of ASC during early phases of neuroinflammation following PNI.[15] Such positive effects were confirmed on nerve histomorphometry, especially nerve fiber density, axon, and myelin area in the ASC-treated group.

Despite their value in reflecting the extent and quality of nerve regeneration, nerve histomorphometry,

gastrocnemius weigh ratios, and electrophysiology suffer from poor correlation or lack functional/behavioral information.[14,15] Indeed, lack of tests combining objective functional motor evaluation with ease of repetitive testing without need for expensive setups is one of the chief limitations in nerve regeneration research.

Reports of systemic use of ASCs in PNI are scarce and, to best of our knowledge, is limited to a single study of a mouse model of sciatic nerve crush injury, which demonstrated improved function on SSI with ASC therapy 1 week after crush injury and improvement in histomorphometric outcomes.[45] No dynamic functional testing was performed.

Although static functional measures such as walking track analysis or treadmills are decades old,[25,52] modifications like the Catwalk XT system have gained popularity in experimental models of PNI[53,54] or neuropathic pain in rodents.[55–57] Although these studies claim that CatWalk can purportedly quantify mechanical allodynia as well as assess subtle alterations across multiple parameters, other studies emphasize its unreliability in PNI.[58,59] One limitation of CatWalk is the need for voluntary locomotion for evaluation of gait parameters. Persistent pain and gravity can limit load bearing. A recent test that has shown promise in overcoming these limitations is the dynamic swim test. This is a measure of global limb functional activity and involuntary motor activity in the absence of gravity. Although the swim test has been used in models of depression or central nervous system injury,[20,21] it has never been evaluated in PNI. We compared functional assessment of animals with resected versus repaired sciatic nerves with CatWalk and swim test and found that both were sensitive enough to detect loss of function after injury, but the CatWalk system was not able to distinguish between "repair" and "no repair" and monitor functional recovery in the early phase of PNI. **(See figure, Supplemental Digital Content 3**, which displays functional analysis using the CatWalk system. After sciatic nerve resection (10 mm; CUT) and sciatic cut and repair (REP), different parameters were recorded over 6 weeks, including BL (preoperative) assessment (X axis). The parameters are divided into static (A) and dynamic (B). The injured side (RH) is compared with the noninjured side (LH) and a ratio is calculated. #$P < 0.05$ vs BL. The CatWalk system is a computed video gait analysis system for quantifying functional recovery. Rats cross a 1.5-m-long and a 10-cm-narrow tunnel with a glass surface and black walls to enter a goal box at the opposite end of the tunnel, and a camera records the runs. The CatWalk system software provides a wide variety of static and dynamic parameters, including the ones we selected for being most appropriate to our setting. "Print length" is defined as the horizontal length of the complete print, and the "print area" is defined as the surface area of the complete print. The CatWalk software creates a rectangular box around each paw print, allowing for measurement of the length and area. "Maximum intensity" reflects the maximum pressure exerted by a single paw and is expressed in arbitrary units. CatWalk further offers parameters that incorporate time measurements for dynamic assessment of functional recovery. The "swing phase" is determined as the duration in which a paw has no detectable contact with the walkway. Contrary to the swing phase, the "stand phase" describes the time of detectable paw contact with the glass plate. A complete step cycle consists of a stand and swing phase. "Single stance" describes the duration of ground contact in seconds for a single paw where the contralateral side does not touch the ground. The "duty cycle" is calculated as: duty cycle = stand/(stand + swing) × 100%, **http://links.lww.com/PRSGO/B424**.)

In our study, infusion of ASCs 1 day after PNI demonstrated beneficial effects in both static and dynamic testing. Early improvement in terms of strokes and swim duration in the first 2 weeks in the ASC group could be interpreted as a result of anti-inflammatory and immunomodulatory function with reduction of postoperative pain, swelling, and reduction of surgical trauma, since clinically relevant nerve regeneration is not expected that early. Our results concur with Marconi et al[45] in the murine nerve crush model. At 6 weeks, swim duration and overall performance score were significantly improved after ASC therapy, while non ASC-treated animals exhibited worse functional return.

Our swim test system is easy to set up, using a commercially available camera, the GoPro. It can be expanded with additional mirrors, sophisticated lighting, and professional recording devices for 3D assessment of complex functional parameters.[20] The buoyancy, absence of gravity, and lack of ground reaction forces acting on the animal's injured leg allow for functional testing with less pain and decreased need of strength, allowing an early detection of functional recovery with less biases.

Study limitations

First, analysis of gastrocnemius weights and histomorphometry occurred only at endpoint, preventing an understanding of the dynamics of early regeneration. In the functional testing, we could see a differential response between both repair groups at early time points (1–3 weeks), which could be explained mechanistically by examination of tissue samples at these time points. Second, the cut/repair model may not be as robust as critical gap models for evaluation of neurotherapies. Third, evaluation of only a single cell dosage and timepoint prevented elucidation of the mechanism by which ASC administration promotes nerve regeneration. Although the current study did not monitor homing of injected cells, our group previously demonstrated that intravenous injected MSCs home to perivascular niches in inflamed tissue (eg, in the setting of critical ischemia).[46] Other groups have reported that cells get entrapped in the lung capillaries after injection but nevertheless exert positive therapeutic effects.[60]

CONCLUSIONS

In summary, our results suggest that early systemic ASC administration is safe and augments nerve regeneration after peripheral nerve transection and repair, resulting in increased motor function compared with nerve repair

without cell therapy. Of note, the SSI outcomes reflected specific reinnervation of the intrinsic muscle of the paw, while the swim test provided an objective assessment of involuntary measures such as hind paw function, tail movement, velocity, forelimb strokes, and hind forelimb coordination. Both SSI and swim test outcomes were supported by gastrocnemius muscle scores and histomorphometry data.

Vijay Gorantla, MD, PhD
Department of Surgery
Wake Forest Baptist Health System
Wake Forest University Health Sciences
Wake Forest Institute for Regenerative Medicine
Suite 333, Technology Drive
Winston Salem, NC 27101
E-mail: vgorantl@wakehealth.edu

REFERENCES

1. Thorsén F, Rosberg HE, Steen Carlsson K, et al. Digital nerve injuries: epidemiology, results, costs, and impact on daily life. *J Plast Surg Hand Surg*. 2012;46:184–190.
2. Taylor CA, Braza D, Rice JB, et al. The incidence of peripheral nerve injury in extremity trauma. *Am J Phys Med Rehabil*. 2008;87:381–385.
3. Tubbs RS, Rizk E, Shoja MM, et al. *Nerves and Nerve Injuries*. Elsevier Ltd, New York; 2015.
4. Scholz T, Krichevsky A, Sumarto A, et al. Peripheral nerve injuries: an international survey of current treatments and future perspectives. *J Reconstr Microsurg*. 2009;25:339–344.
5. Kuffler DP. Promoting axon regeneration and neurological recovery following traumatic peripheral nerve injuries. *Int J Neurorehabilitation*. 2015;2:1–17.
6. Rotshenker S. Wallerian degeneration: the innate-immune response to traumatic nerve injury. *J Neuroinflammation*. 2011;8:109.
7. Kingham PJ, Kalbermatten DF, Mahay D, et al. Adipose-derived stem cells differentiate into a Schwann cell phenotype and promote neurite outgrowth *in vitro*. *Exp Neurol*. 2007;207:267–274.
8. di Summa PG, Kingham PJ, Raffoul W, et al. Adipose-derived stem cells enhance peripheral nerve regeneration. *J Plast Reconstr Aesthet Surg*. 2010;63:1544–1552.
9. Erba P, Mantovani C, Kalbermatten DF, et al. Regeneration potential and survival of transplanted undifferentiated adipose tissue-derived stem cells in peripheral nerve conduits. *J Plast Reconstr Aesthet Surg*. 2010;63:e811–e817.
10. Zheng L, Cui HF. Use of chitosan conduit combined with bone marrow mesenchymal stem cells for promoting peripheral nerve regeneration. *J Mater Sci Mater Med*. 2010;21:1713–1720.
11. Sun F, Zhou K, Mi WJ, et al. Repair of facial nerve defects with decellularized artery allografts containing autologous adipose-derived stem cells in a rat model. *Neurosci Lett*. 2011;499:104–108.
12. Yang Y, Yuan X, Ding F, et al. Repair of rat sciatic nerve gap by a silk fibroin-based scaffold added with bone marrow mesenchymal stem cells. *Tissue Eng Part A*. 2011;17:2231–2244.
13. Lin YC, Oh SJ, Marra KG. Synergistic lithium chloride and glial cell line-derived neurotrophic factor delivery for peripheral nerve repair in a rodent sciatic nerve injury model. *Plast Reconstr Surg*. 2013;132:251e–262e.
14. Kappos EA, Engels PE, Tremp M, et al. Peripheral nerve repair: multimodal comparison of the long-term regenerative potential of adipose tissue-derived cells in a biodegradable conduit. *Stem Cells Dev*. 2015;24:2127–2141.
15. Tremp M, Sprenger L, Degrugillier L, et al. Regeneration of nerve crush injury using adipose-derived stem cells: a multimodal comparison. *Muscle Nerve*. 2018;58:566–572.
16. di Summa PG, Kalbermatten DF, Raffoul W, et al. Extracellular matrix molecules enhance the neurotrophic effect of Schwann cell-like differentiated adipose-derived stem cells and increase cell survival under stress conditions. *Tissue Eng Part A*. 2013;19:368–379.
17. Di Summa PG, Schiraldi L, Cherubino M, et al. adipose derived stem cells reduce fibrosis and promote nerve regeneration in rats. *Anat Rec (Hoboken)*. 2018;301:1714–1721.
18. Sabol RA, Bowles AC, Cote A, et al. Therapeutic potential of adipose stem cells. *Adv Exp Med Biol*. 2018. [Epub ahead of print]
19. De Francesco F, Ricci G, D'Andrea F, et al. Human adipose stem cells: from bench to bedside. *Tissue Eng Part B Rev*. 2015;21:572–584.
20. Zörner B, Filli L, Starkey ML, et al. Profiling locomotor recovery: comprehensive quantification of impairments after CNS damage in rodents. *Nat Methods*. 2010;7:701–708.
21. Xu N, Åkesson E, Holmberg L, et al. A sensitive and reliable test instrument to assess swimming in rats with spinal cord injury. *Behav Brain Res*. 2015;291:172–183.
22. Plock JA, Schnider JT, Schweizer R, et al. The influence of timing and frequency of adipose-derived mesenchymal stem cell therapy on immunomodulation outcomes after vascularized composite allotransplantation. *Transplantation*. 2017;101:e1–e11.
23. Plock JA, Schnider JT, Zhang W, et al. Adipose- and bone marrow-derived mesenchymal stem cells prolong graft survival in vascularized composite allotransplantation. *Transplantation*. 2015;99:1765–1773.
24. Badia J, Pascual-Font A, Vivó M, et al. Topographical distribution of motor fascicles in the sciatic-tibial nerve of the rat. *Muscle Nerve*. 2010;42:192–201.
25. Bervar M. Video analysis of standing—an alternative footprint analysis to assess functional loss following injury to the rat sciatic nerve. *J Neurosci Methods*. 2000;102:109–116.
26. Kostereva NV, Wang Y, Fletcher DR, et al. IGF-1 and chondroitinase ABC augment nerve regeneration after vascularized composite limb allotransplantation. *PLoS One*. 2016;11:e0156149.
27. Barry FP, Murphy JM. Mesenchymal stem cells: clinical applications and biological characterization. *Int J Biochem Cell Biol*. 2004;36:568–584.
28. Baer PC, Geiger H. Adipose-derived mesenchymal stromal/stem cells: tissue localization, characterization, and heterogeneity. *Stem Cells Int*. 2012;2012:812693.
29. Chu DT, Nguyen Thi Phuong T, Tien NLB, et al. Adipose tissue stem cells for therapy: an update on the progress of isolation, culture, storage, and clinical application. *J Clin Med*. 2019;8:E917.
30. Zack-Williams SD, Butler PE, Kalaskar DM. Current progress in use of adipose derived stem cells in peripheral nerve regeneration. *World J Stem Cells*. 2015;7:51–64.
31. De la Rosa MB, Kozik EM, Sakaguchi DS. Adult stem cell-based strategies for peripheral nerve regeneration. *Adv Exp Med Biol*. 2018;1119:41–71.
32. Ohta Y, Hamaguchi A, Ootaki M, et al. Intravenous infusion of adipose-derived stem/stromal cells improves functional recovery of rats with spinal cord injury. *Cytotherapy*. 2017;19:839–848.
33. Ching RC, Wiberg M, Kingham PJ. Schwann cell-like differentiated adipose stem cells promote neurite outgrowth via secreted exosomes and RNA transfer. *Stem Cell Res Ther*. 2018;9:266.
34. Tse KH, Novikov LN, Wiberg M, et al. Intrinsic mechanisms underlying the neurotrophic activity of adipose derived stem cells. *Exp Cell Res*. 2015;331:142–151.
35. Sowa Y, Kishida T, Imura T, et al. Adipose-derived stem cells promote peripheral nerve regeneration *in vivo* without

differentiation into Schwann-like lineage. *Plast Reconstr Surg.* 2016;137:318e–330e.
36. Raisi A, Azizi S, Delirezh N, et al. The mesenchymal stem cell-derived microvesicles enhance sciatic nerve regeneration in rat: a novel approach in peripheral nerve cell therapy. *J Trauma Acute Care Surg.* 2014;76:991–997.
37. Watanabe Y, Sasaki R, Matsumine H, et al. Undifferentiated and differentiated adipose-derived stem cells improve nerve regeneration in a rat model of facial nerve defect. *J Tissue Eng Regen Med.* 2017;11:362–374.
38. Orbay H, Uysal AC, Hyakusoku H, et al. Differentiated and undifferentiated adipose-derived stem cells improve function in rats with peripheral nerve gaps. *J Plast Reconstr Aesthet Surg.* 2012;65:657–664.
39. Saller MM, Huettl RE, Mayer JM, et al. Validation of a novel animal model for sciatic nerve repair with an adipose-derived stem cell loaded fibrin conduit. *Neural Regen Res.* 2018;13:854–861.
40. di Summa PG, Kingham PJ, Campisi CC, et al. Collagen (NeuraGen®) nerve conduits and stem cells for peripheral nerve gap repair. *Neurosci Lett.* 2014;572:26–31.
41. Reichenberger MA, Mueller W, Hartmann J, et al. ADSCs in a fibrin matrix enhance nerve regeneration after epineural suturing in a rat model. *Microsurgery.* 2016;36:491–500.
42. Hsueh YY, Chang YJ, Huang TC, et al. Functional recoveries of sciatic nerve regeneration by combining chitosan-coated conduit and neurosphere cells induced from adipose-derived stem cells. *Biomaterials.* 2014;35:2234–2244.
43. Matthes SM, Reimers K, Janssen I, et al. Intravenous transplantation of mesenchymal stromal cells to enhance peripheral nerve regeneration. *Biomed Res Int.* 2013;2013:573169.
44. Eggenhofer E, Benseler V, Kroemer A, et al. Mesenchymal stem cells are short-lived and do not migrate beyond the lungs after intravenous infusion. *Front Immunol.* 2012;3:297.
45. Marconi S, Castiglione G, Turano E, et al. Human adipose-derived mesenchymal stem cells systemically injected promote peripheral nerve regeneration in the mouse model of sciatic crush. *Tissue Eng Part A.* 2012;18:1264–1272.
46. Schlosser S, Dennler C, Schweizer R, et al. Paracrine effects of mesenchymal stem cells enhance vascular regeneration in ischemic murine skin. *Microvasc Res.* 2012;83:267–275.
47. Schweizer R, Kamat P, Schweizer D, et al. Bone marrow-derived mesenchymal stromal cells improve vascular regeneration and reduce leukocyte-endothelium activation in critical ischemic murine skin in a dose-dependent manner. *Cytotherapy.* 2014;16:1345–1360.
48. Kalbermatten DF, Schaakxs D, Kingham PJ, et al. Neurotrophic activity of human adipose stem cells isolated from deep and superficial layers of abdominal fat. *Cell Tissue Res.* 2011;344:251–260.
49. Mahay D, Terenghi G, Shawcross SG. Schwann cell mediated trophic effects by differentiated mesenchymal stem cells. *Exp Cell Res.* 2008;314:2692–2701.
50. Nijhuis TH, de Boer SA, de Boer SA, et al. A new approach to assess the gastrocnemius muscle volume in rodents using ultrasound; comparison with the gastrocnemius muscle index. *PLoS One.* 2013;8:e54041.
51. Yu X, Bellamkonda RV. Tissue-engineered scaffolds are effective alternatives to autografts for bridging peripheral nerve gaps. *Tissue Eng.* 2003;9:421–430.
52. Tomita K, Nishibayashi A, Yano K, et al. Adipose-derived stem cells protect against endoneurial cell death: cell therapy for nerve autografts. *Microsurgery.* 2015;35:474–480.
53. Bozkurt A, Deumens R, Scheffel J, et al. CatWalk gait analysis in assessment of functional recovery after sciatic nerve injury. *J Neurosci Methods.* 2008;173:91–98.
54. Chiang CY, Sheu ML, Cheng FC, et al. Comprehensive analysis of neurobehavior associated with histomorphological alterations in a chronic constrictive nerve injury model through use of the CatWalk XT system. *J Neurosurg.* 2014;120:250–262.
55. Vrinten DH, Hamers FF. "CatWalk" automated quantitative gait analysis as a novel method to assess mechanical allodynia in the rat; a comparison with von Frey testing. *Pain.* 2003;102:203–209.
56. Gabriel AF, Marcus MA, Walenkamp GH, et al. The CatWalk method: assessment of mechanical allodynia in experimental chronic pain. *Behav Brain Res.* 2009;198:477–480.
57. Sakuma T, Kamoda H, Miyagi M, et al. Comparison of CatWalk analysis and von Frey testing for pain assessment in a rat model of nerve crush plus inflammation. *Spine (Phila Pa 1976).* 2013;38:E919–E924.
58. Kappos EA, Sieber PK, Engels PE, et al. Validity and reliability of the CatWalk system as a static and dynamic gait analysis tool for the assessment of functional nerve recovery in small animal models. *Brain Behav.* 2017;7:e00723.
59. Deumens R, Jaken RJ, Marcus MA, et al. The CatWalk gait analysis in assessment of both dynamic and static gait changes after adult rat sciatic nerve resection. *J Neurosci Methods.* 2007;164:120–130.
60. Lee RH, Pulin AA, Seo MJ, et al. Intravenous hMSCs improve myocardial infarction in mice because cells embolized in lung are activated to secrete the anti-inflammatory protein TSG-6. *Cell Stem Cell.* 2009;5:54–63.